증기상 중합을 통한 기체/물 계면에서 전도성 프리스탠딩 필름의 성장 메커니즘에 관한 연구

Kerguelen Mae Nodora · 임진형[†]

공주대학교 공과대학 신소재공학부

Study of Growth Mechanism of Conductive Free-standing Films on a Vapor/Water Interface via Gas Phase Polymerization

Kerguelen Mae Nodora and Jin-Heong Yim[†]

Division of Advanced Materials Engineering, Kongju National University
1223-24 Cheoandaero, Cheonan, Chungnam 31080, Korea

초록: 증기/수용액 계면에서 두 종류의 다른 층을 가지는 전도성 하이브리드 프리스탠딩 필름을 제조하였다. 폴리피롤(PPy)-SiO₂ 및 PPy-폴리(3,4-에틸렌 디옥시 티오펜)(PEDOT) 프리스탠딩 필름은 기체/물 계면에서 가스상의 단량체와 수용액상의 산화제의 접촉으로 인한 산화-커플링 계면중합을 통한 순차적 기상 중합(consecutive-vapor phase polymerization; c-VPP) 방법으로 합성되었다. 제조된 하이브리드 프리스탠딩 필름은 유연하고 견고하며 기판이 존재하지 않더라도 그 구조를 유지할 수 있었다. 복합체의 화학조성과 형태학적 분석으로부터 단량체 기체가 초기 형성된 폴리머 층으로 확산되어 활성 산화제에 도달하여 사슬 성장을 위한 중합이 진행되는 하향식(top-down) 성장 메커니즘에 대한 증거를 제공하였다. c-VPP의 다양한 제조 조건(중합 순서, 단량체의 종류, 중합 시간)을 조절하여 제조된 하이브리드 프리스탠딩 필름의 화학적 조성과 전기적 특성을 효과적으로 조절할 수 있었다.

Abstract: In this paper, two kinds of conductive hybrid free-standing films (polypyrrole (PPy)-SiO₂ and PPy-poly(3,4-ethylenedioxythiophene) (PEDOT) hybrid) were successfully prepared by employing the consecutive vapor phase polymerization (c-VPP) technique. Through the spontaneous interface polymerization of the monomer gas molecules in the vapor/aqueous interface of the oxidant in water, free-standing films were synthesized via oxidative-coupling polymerization. The as-prepared free-standing films were flexible to a certain degree, robust, and can maintain their structure even without any support of donor substrates. Importantly, chemical compositional and morphological analyses on the top-side and bottom-side surface of the films provided evidence for a top-down growth mechanism in which the arriving monomer vapors diffuse to the initially formed polymer product layer to reach active oxidant film for chain growth. Intricate film morphology and the electrical properties of the films can be effectively adjusted by controlling the order of monomer polymerization, the type of monomers to be used, and the polymerization time in each monomer chamber.

Keywords: consecutive vapor phase polymerization, free-standing hybrid, film growth mechanism, vapor/water interface polymerization.

Introduction

Since the highly successful discovery of conducting polymers (CPs), also known as conjugated polymers, in the late 1970 s,[1] widespread applications have been discovered due to their high conductivity, compatibility, and easy processability.[2-4]

Numerous types of CPs (e.g., poly(3,4-ethylenedioxythiophene) (PEDOT), polypyrrole (PPy), polythiophene, and polyaniline have been developed which opened a new array of possibilities for almost any desired applications such as in biomedical applications,[5] strain sensors,[6,7] chemical sensors,[8-10] "green electronics",[11] and in solar cells.[12] Regarding the conductive polymers, PEDOT and PPy, and their derivatives are frequently employed in various applications.[13,14] Free-standing conductive films have attracted a great interest due to its high

potential in various applications such as in high-performance energy devices,[15] biomedical devices, for instance, bio-hybrid actuating devices,[16] flexible thermoelectric devices,[17] and nanowire films for supercapacitors.[18] With these technological advancements, there is a need to have a deeper understanding of how conductive free-standing films propagate and grow during the fabrication process; in this case, the method employed in producing free-standing films is vapor phase polymerization (VPP). In this given the circumstances, there would be a question regarding the controversial layer growth mechanism on how conductive polymers grow, specifically on a vapor/water interface, during VPP. According to previous studies, there are two recognized growth mechanisms surrounding intrinsically CPs on thin films growth; top-down process[19-21] and the bottom-up process.[22-25] A top-down approach is a type of mechanism in which the polymerization takes place on the surface of the oxidant or the bulk oxidant, it is also called monomer diffusion because the monomer diffuses through the recently formed polymer layer to reach the oxidant for polymerization.[20] While the bottom-up process, or oxidant diffusion, the oxidant layer migrates upward through the forming polymer layer by means of capillary action. The movement of this oxidant layer served as a replenishment to the spent oxidant used by the initially formed polymer layer.[22,23]

In this work, the growth mechanism of the fabricated free-standing PPy-SiO$_2$ and PPy-PEDOT films polymerized on a vapor/water interface via the consecutive-VPP (c-VPP) method is demonstrated. The sequential polymerization of the PPy film followed the SiO$_2$ film will provide the evidence as to what type of growth mechanism is occurring during the process. To provide a more coherent report, the procedure is repeated for reversed polymerization, tetraethyl orthosilicate (TEOS) followed by pyrrole (Py) monomer. Moreover, the growth mechanism organic-organic PPy-PEDOT free-standing film was also analyzed. The second aim of this paper is to provide a facile method to synthesize hybrid conductive free-standing films through the process of c-VPP. The free-standing films were analyzed for electrical properties, surface, and cross-sectional components and to further understand the formation mechanism, the films were characterized by energy dispersive spectroscopy (EDS) elemental mapping as well as surface morphological analysis.

Experimental

Materials. TEOS (Samchun Pure Chemical Co., Seoul, Korea) as a precursor for silica-based inorganic network structure, Py (Acros Organics, New Jersey, USA) as a precursor for PPy, 3,4-ethylenedioxythiophene (EDOT) (Sigma-Aldrich, St. Louis, MO, USA) as the monomer for PEDOT, Iron (III) chloride hexahydrate (FeCl$_3$·6H$_2$O) (Sigma-Aldrich, St. Louis, MO, USA) as the oxidizing agent and dopant were used without further purification.

Fabrication of PPy-SiO$_2$ and PPy-PEDOT Free-standing Thin Films. To prepare PPy-SiO$_2$ free-standing thin films, 0.41 g of FeCl$_3$·6H$_2$O was diluted in 3 mL distilled water in a petri dish (31.5 mm in diameter) to prepare 0.5 M FeCl$_3$ aqueous solution. Chemical polymerization of Py would be a reasonable approach when Iron (III) chloride and water are used as the oxidizing agent and solvent respectively in terms of conductivity characteristics.[26-28] The prepared oxidant solution in the petri dish is sequentially polymerized with Py vapor at ambient conditions for 1 and 3 h and immediately thereafter exposed to TEOS vapor at 60 °C for 3 and 1 h respectively as described in Scheme 1(a). The total polymerization time in the two chambers is 4 h. To avoid conjectures and to closely analyze the growth mechanism of free-standing films prepared on a vapor/water interface via c-VPP, the order in which monomers are polymerized was also reversed in which TEOS was first polymerized immediately followed by Py polymerization (Scheme 1(b)). Apart from this, another type of monomer, EDOT monomer instead of TEOS, was used (Scheme 1(c), 1(d)). The same process was applied as well. Note the different temperature levels in each monomer chamber were necessary due to their different vapor pressures. Through the spontaneous interface polymerization of the monomer gas in the vapor/water interface of the FeCl$_3$-oxidant in water,[28] free-standing films PPy-SiO$_2$ and PPy-PEDOT were developed. The generated free-standing films were carefully peeled off using a tweezer. The order of the monomer being polymerized as well as the polymerization time in the chambers will provide conclusive evidence as to what type of growth mechanism exists in preparing the free-standing films. Nomenclatures of the films are defined as shown in Scheme 1(e). P, T, and E stand for Py, TEOS, and EDOT monomer, respectively while the subscripts oo and xx are the polymerization time in each chamber. PT series are a set of films in which Py was first polymerized followed by TEOS and if the order of polymerization is reversed TP series films are produced. PE series is a set of films in which Py was first polymerized followed by EDOT and if the order of polymerization is reversed EP series films are produced.
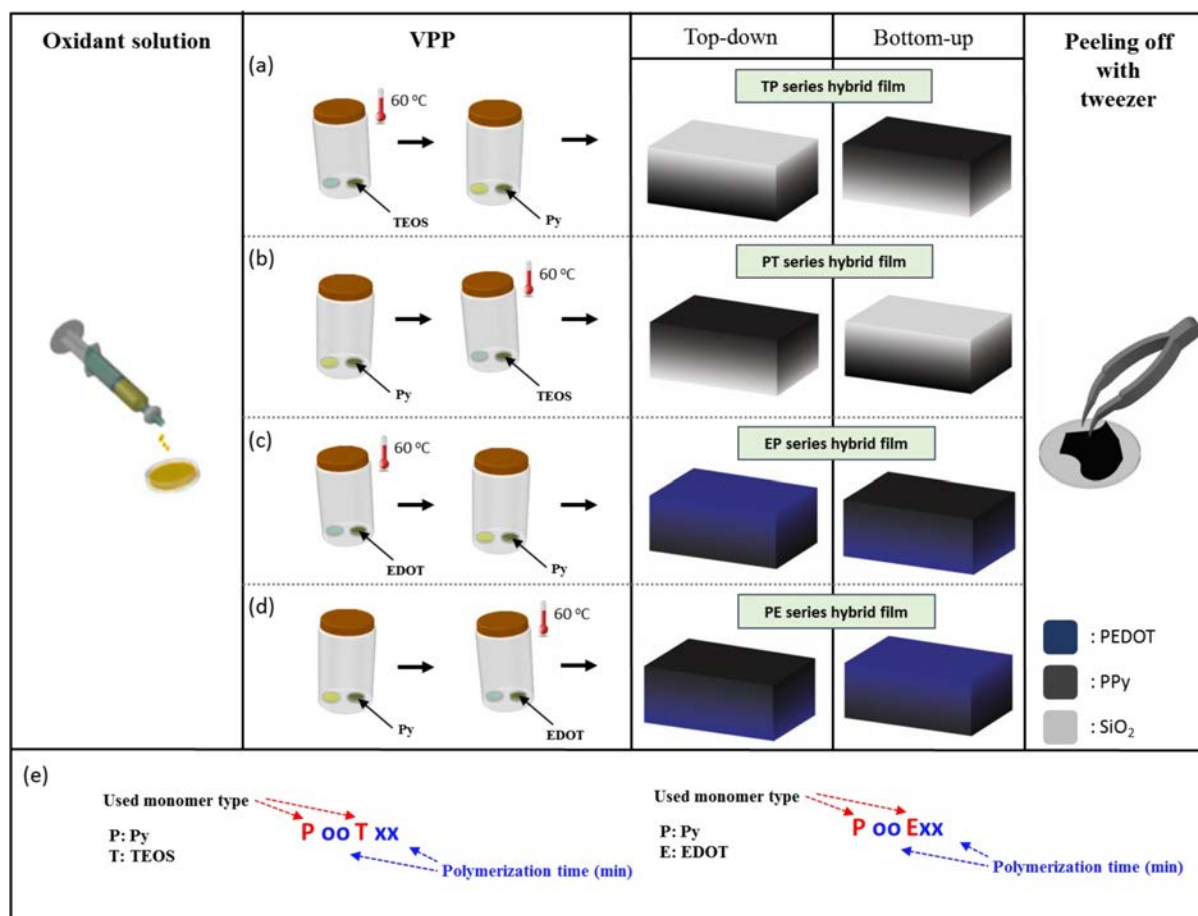
Scheme 1. The fabrication process for stepwise VPP for making conceptually two-layered PPy-SiO$_2$ and PPy-PEDOT free-standing films on plausible two different film growth mechanism: (a) TP series hybrid films; (b) PT series hybrid films; (c) EP series hybrid films; (d) PE series hybrid films; (e) abbreviation definition of prepared composite material..

Measurement and Analysis. The resistivity of the films was measured by a multi-meter (HIOKI 3280-10F, Japan) in which silver paste was used as electrodes on both sides of the film. Bending tests were conducted to confirm the mechanical robustness of the free standing films using an in-house multipurpose flexibility test machine (IPEN Co., Korea). The morphologies of the surface and cross-section of the thin films were observed using field emission scanning electron microscope (FE-SEM) systems (TESCAN, MIRA LMH, Czech). The chemical composition of each surface for various free-standing film was analyzed using Energy-dispersive spectroscopy elemental mapping (EDS, Bruker AXS XFlash detector 5010, USA).

Results and Discussion

Fabrication and Electro-mechanical Property Analysis

of Free-standing PPy-SiO$_2$ and PPy-PEDOT Hybrid Films. Free-standing films were fabricated through c-VPP of assigned monomers as outlined in Scheme 1. Sequential polymerization in the vapor/water interface was used to prepare two-layered organic-inorganic and organic-organic free-standing films, PPy-SiO$_2$ and PPy-PEDOT films respectively. The term conductive organic-inorganic hybrid film is an integrated concept of polymerized electro-conductive organic monomers such as EDOT and Py and metal alkoxide precursors such as silicon, aluminum, titanium alkoxides. Insights regarding the growth mechanism of these films would help in modifying and tuning the properties and morphology of the as-prepared films. To render a comprehensive report, the growth mechanism for both organic-organic and organic-inorganic free-standing films were analyzed and differentiated. From Figure 1(a), it is regarded that the produced film, after the 4 h polymerization in 2 monomer chambers, is black in color and has a relatively uniform
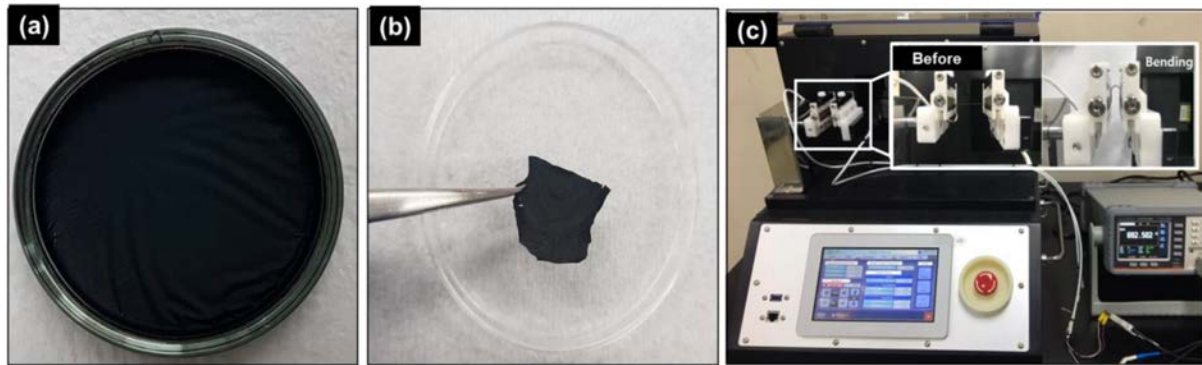
Figure 1. (a) Digital photo of the film in a petri-dish still containing the unreacted oxidant solution; (b) the film prepared with 0.5 M FeCl$_3$ peeled off by tweezers after 4 h of sequential polymerization; (c) repeated bending experiment of a free standing film.

and sleek appearance on the top of the oxidant solution in the petri dish. This simply signifies that polymerization took place on the entire surface of the bulk oxidant solution. These kinds of physical features are apparent for all sets of films regardless of the types of monomer used, the time of polymerization in each chamber, and the order of polymerization. The resulting films can be carefully peeled off from the oxidant solution with the use of tweezer as shown in Figure 1(b). What's left behind is the unreacted and unused oxidant aqueous solution. The peeling off process is a good indicator that the film is flexible to a certain degree and is robust, and can exist and maintain the structure even without the use of a substrate as reported in the previous literature.[28] Moreover, the film did not change in shape even in repeated bending experiment over 100 times using our in-house multipurpose flexibility test machine as shown in Figure 1(c).

The comparison of the relative resistances of the free-standing films prepared with different polymerization conditions is presented in Figure 2. The pristine PPy film (P4), which resulted from 4 h polymerization in the Py chamber, displayed the lowest resistance among the other films. With the incorporation of SiO$_2$ in the Py matrix, such as P1T3 and T3P1, the resistance of the films was significantly increased by about three times. The reason for the increase in resistance for PT/TP series samples can be attributed to the existence of SiO$_2$ polymerized from the TEOS chamber, and it is known that SiO$_2$ is an electrically insulating material, a type of material that does not readily allow the flow of electrons in the polymer matrix. The polymerization order in the TEOS and Py chamber is not an important parameter, thus contributing to the slight increase in the resistance of the T3P1/P1T3 films. Therefore, merging an insulating domain to an electrically conductive
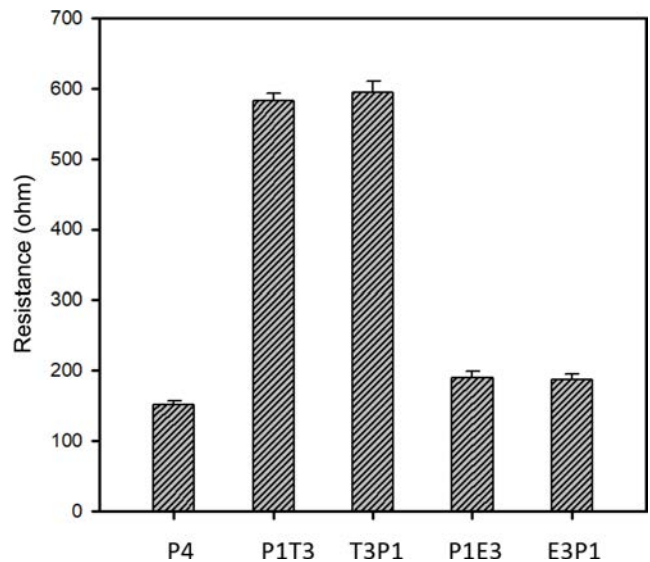
Figure 2. Relative resistivity of various free-standing films prepared at different polymerization conditions, resistance was measured using digital multi-meter and silver paste as electrodes.

polymer is the key factor in the sudden increase in resistance. Conversely, there was a discernible slight increase in the resistance for films under PE series, as represented by P1E3 and E3P1, in reference to pristine PPy film. This slight increase might be due to the contact resistance from the existence of interface between PEDOT and PPy domains. These kinds of hybrid could have potentials because it can be tunable bandgap of these two known highly conductive polymers, namely PEDOT and PPy. Reports revealed the PEDOT exhibits a bandgap of 1.6-1.7 eV[29] while pristine PPy has a lower bandgap of 1.37 eV.[30] These findings suggest that synergistic combinations of two or more different monomers can tune or control the electrical properties and other characteristics of the

films depending on the requirements on certain applications.

Morphological/Chemical Compositional Analysis of Free-standing Films. Over the course of c-VPP, there should be close interaction between the arriving monomers and the oxidant solution, and with these two schemes are possible to develop: oxidant diffusion via upward capillary movement (bottom-up process[22-25]) or monomer diffusion via downward diffusion (top-down process).[19-21] Subsequent to the different monomer deposition and polymerization conditions, the surface morphologies of the top side and the bottom side of the films were determined by SEM (Figure 3). The SEM images revealed porous structures across the surface of the top side of the films under PT/TP series (Figure 3(a) and 3(b)). Such porous structures were also observed for pristine free-standing Py wherein the apportionment of pore diameter ranges from 4 to 15 μm for 0.5 M $FeCl_3$ concentration as reported previously.[28] As compared with P1T3 (Figure 3(a)), the topside surface of T3P1 (Figure 3(b)) exhibited smaller micro-size pores and even more circular and regular in shape. It is found that when TEOS was first polymerized followed by Py, smoother and small pores are detected because the initially formed SiO_2 layer has the tendency to provide exterior smoothness[31] and the sol-gel of SiO_2 impedes the polymerization rate of Py.[32] This suggests that the layer in the topside part of T3P1 could be more like SiO_2. By contrast, when the order of monomer introduction was swapped, in which Py was first polymerized followed by TEOS, the topside surface of T1P3 appears to have pores with an irregular shape that implies that the layer in the topside of the film might be relatively PPy-rich area. More-

over, this part of the film has larger pores because as the polymerization reaction proceeds, the Py at the upper surface of the film becomes drier leaving larger holes.[28] The SEM images of the bottom side of the PT/TP films are also shown in Figure 3(a′) and 3(b′). Compared to the surfaces of the topside, the bottom part of the PT/TP series seems to have appearances like agglomerate of small granular microparticles. This suggests that these parts of the films exposed to the oxidant solution are more hydrated compared to the upper surface and as a result, more irregular surface morphologies are observed. The SEM images of the topside surface of EP/PE films are shown in Figure 3(c) and 3(d), respectively. Few tiny pinhole defects along the grainy surface are observed on the topside surface of P1E3 (Figure 3(c)). These tiny pinholes or porous structures are indications that this polymer layer situated on the upper surface of P1E3 might be of PPy-rich area. On the contrary, the topside surface of E3P1 shows a solid heterogeneous surface with some degree of roughness having non-porous structures, a typical surface morphology of VPP based PEDOT film.[33] The SEM images of the bottom side of the PT/TP films are also shown in Figure 3(c′) and 3(d′), having small granular appearances due to its waterish features.[28] The differences in the morphologies of these films can be attributed to the different interactions between monomers during film formation. SEM analysis suggests that during c-VPP in vapor/water interface, a top-down growth mechanism exists, during which the monomer diffuses through the recently formed polymer layer to reach the bulk oxidant.

The growth mechanism of organic-inorganic (PT/TP films)
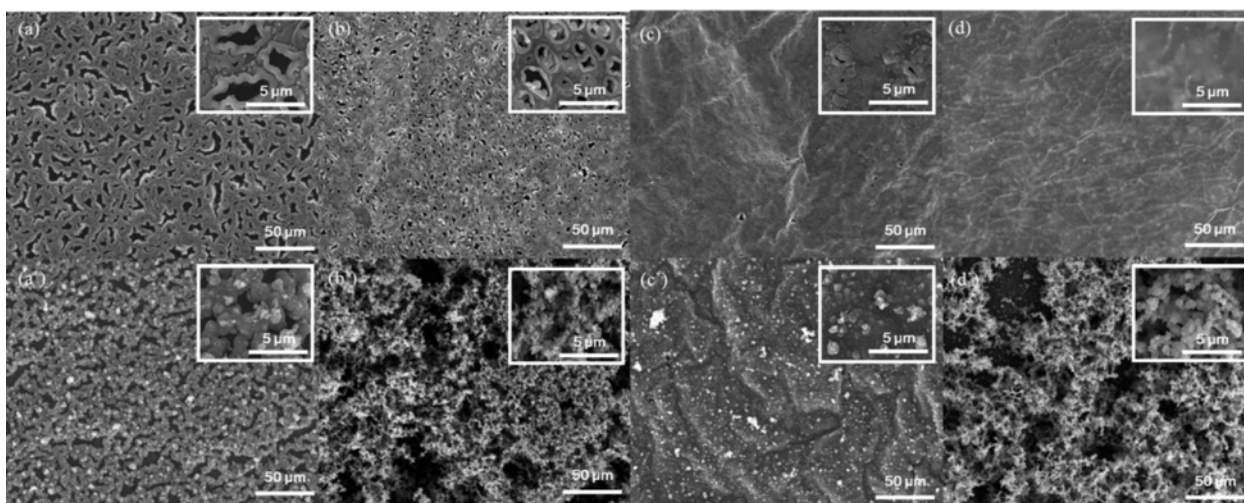
Figure 3. SEM images of various free-standing films, upside and downside respectively: (a and a') P1T3; (b and b') T3P1; (c and c') P1E3; (d and d') E3P1.

and organic-organic (PE/EP films) free-standing films are verified in order to provide a more coherent report if the type and nature of monomers used in VPP may affect how polymers grow during the said process. To further validate that a top-down mechanism exists during the VPP in the vapor/water interface, EDS elemental analysis, both at the topside and bottom side, has been employed. If the top-down growth mechanism transpires during c-VPP, in the case of P1T3, after the Py monomer used the oxidant at the water/vapor interface for initial polymer growth, the introduction of the second monomer which is TEOS would cause it to diffuse to the recently formed PPy later to reach the underling oxidant for polymerization. This would lead to the topside being PPy-rich and SiO_2-rich for the bottom side. The converse is true for T3P1 films, wherein the sequential polymerization of monomers was reversed. The same manner would be observed for P1E3 and E3P1 if the top-down mechanism would be true. The results of the chemical compositional analysis by EDS investigation on the topside and bottom side of the PT/TP and PE/EP films are presented in Table 1 and Table 2, respectively. The calculated SiO_2 content on the topside (0.45%) and bottom side (3.42%) of P1T3, as shown in Table 1, proposes that the topside is more PPy-like whereas the bottom side is more SiO_2-like. Furthermore, the PPy/SiO_2 ratio at the topside of P1T3 is 8 times higher compared to that of the bottom side which implies that

the topside layer is indeed PPy. On the contrary to that, the reverse was observed for T3P1. The SiO_2 content, at the top side of this film is slightly higher than that of the bottom side, with values of 2.43% and 2.02%, respectively. The PPy/SiO_2 ratio at the topside of T3P1 is relatively smaller compared with that of at the bottom side. These results imply that SiO_2 is stationed above the subsequent layers of PPy. As presented in Table 2, the calculated PEDOT content on the bottom side of P1E3 (4.24%), which is comparably higher compared to that of the topside (3.77%), indicates that PEDOT layer is positioned underneath. The reverse was observed for E3P1 in which the PPy layer is positioned below the initially formed PEDOT layer. EDS chemical compositional data also supports the idea of a top-down growth mechanism during c-VPP on the water/vapor interface. The reason for this is that since the oxidant solution is an aqueous media, the oxidant matter was trapped within the solvent molecules, in this case is water, which prevents it from moving or diffusing to generating hydrophobic solid layer, and as a result in order for the polymerization to take place, the monomer moves downward to reach to bulk oxidant. These substantiate the previous findings of Nair et al.[19,20] during the PEDOT growth on a nonwoven porous mat of polystyrene wherein in ferric p-toluenesulfonate oxidant is contained within the nanofibers template and with that, the diffusion of EDOT monomer through the formed

Table 1. Relative Surface Compositions Top Side and Bottom Side of PPy and SiO_2 in the Prepared Free-standing Film by means of EDS Analysis

	Sample	N (atomic%)	Si (atomic%)	N/Si ratio	Calculated PPy/SiO_2 ratio[a]	Calculated SiO_2 content (%)[b]
Topside	P1T3	16.5	0.08	206.3	222.8	0.45
	T3P1	15.6	0.43	36.3	39.2	2.43
Bottomside	P1T3	16.2	0.62	26.1	28.2	3.42
	T3P1	17.5	0.39	44.9	48.5	2.02

[a]Calculated PPy/SiO_2 ratio = N/Si ratio × (repeating unit mass of PPy/repeating unit mass of SiO_2 repeating unit mass of PPy/repeating unit mass of SiO_2 = 65 g (C_4H_2NH)/60 g (SiO_2) = 1.08]. [b]Calculated SiO_2 content (%) = [1/(1 + Calculated PPy/SiO_2 ratio)] × 100.

Table 2. Relative Surface Compositions Top Side and Bottom Side of PPy and PEDOT in the Prepared Free-standing Film by means of EDS Analysis

	Sample	N (atomic%)	S (atomic%)	N/S ratio	Calculated PPy/PEDOT ratio[a]	Calculated PEDOT content (%)[b]
Topside	P1E3	16.5	0.30	55.0	25.5	3.77
	E3P1	13.8	0.28	49.3	22.9	4.18
Bottomside	P1E3	14.6	0.30	48.7	22.6	4.24
	E3P1	15.0	0.26	57.7	26.8	3.60

[a]Calculated PPy/PEDOT ratio = N/S ratio × (repeating unit mass of PPy/repeating unit mass of PEDOT repeating unit mass of PPy/repeating unit mass of PEDOT = 65 g (C_4H_2NH)/140 g ($C_6H_4O_2S$) = 0.464]. [b]Calculated PEDOT content (%) = [1/(1 + Calculated PPy/PEDOT ratio)] × 100.

PEDOT product layer is necessary in order to further continue the polymerization process. A top-down growth mechanism has also been observed in the formation of free-standing PPy films generated on the interface of Py monomer and FeCl₃-oxidant solution in water. The polymerization took place on the vapor/water interface forming a thin layer of PPy film and with continued polymerization, the Py vapor permeates through this initially formed PPy film to reach the FeCl₃ and react, thus, generating another PPy film beneath the existing layer.[28] Taken together, these findings suggest that the monomer is adsorbed on the oxidant solution for chain growth, which leads to the formation of that monomer's polymer layer onto the surface of the oxidant film. The adsorbed monomer then diffuses through this thin polymer layer in order to attain the active oxidant film for polymerization.

Conclusions

In conclusion, this paper has proposed a facile synthesis mechanism for the formation of hybrid conductive free-standing films at the interface of vapor monomers and oxidant solution. This type of method is a variation to the c-VPP technique in which PPy-SiO₂ and PPy-PEDOT hybrid conductive films were successfully fabricated by sequentially polymerizing Py and TEOS and Py and EDOT, respectively on the FeCl₃-oxidant in water. Tunable characteristics and film morphology have also been demonstrated. This approach would lend itself well for large-scale fabrication of uniform and large-area conductive free-standing films with intricate film architecture that are advantageous for numerous applications. In addition, the pieces of evidence from this study intimates a top-down growth mechanism, wherein the monomer vapor diffuses through the existing polymer layer to reach the oxidant film for chain growth by means of downward diffusion for the formation of free-standing films formed through the sequential polymerization of two monomers via c-VPP technique. Regardless of the type of monomers used, whether it's an organic or inorganic monomer the same mechanism applies.

References

1. Chiang, C. K.; Fincher, C. R. Jr.; Park, Y. W.; Heeger, A. J.; Shirakawa, H.; Louis, E. J.; Gau, S. C.; MacDiarmid, A. G. Electrical conductivity in doped polyacetylene. *Phys. Rev. Lett.* **1977**, 39, 1098-1101.

2. Atesa, M.; Karazehira, T.; Saracb, A. S. Conducting Polymers and their Applications. *Curr. Phys. Chem.* **2012**, 2, 224-240.

3. He, H.; Zhang, L.; Guan, X.; Cheng, H.; Liu, X.; Yu, S.; Wei, J.; Ouyang, J. Biocompatible Conductive Polymers with High Conductivity and High Stretchability. *ACS Appl. Mater. Interfaces* **2019**, 11, 26185-26193.

4. Nguyen, D. N.; Yoon, H. Recent Advances in Nanostructured Conducting Polymers: from Synthesis to Practical Applications. *Polymers* **2016**, 8, 118-156.

5. Kaur, G.; Adhikari, R.; Cass, P.; Bown, M.; Evans, M. D. M.; Vashi, A. V.; Gunatillake, P. Graphene/Polyurethane Composites: Fabrication and Evaluation of Electrical Conductivity, Mechanical Properties and Cell Viability. *RSC Adv.* **2015**, 5, 98762-98772.

6. Losaria, P. M.; Yim, J. -H. A Highly Stretchable Large Strain Sensor Based on PEDOT–Thermoplastic Polyurethane Hybrid Prepared via *In Situ* Vapor Phase Polymerization. *J. Ind. Eng. Chem.* **2019**, 71, 108-117.

7. Losaria, P. M.; Yim, J.-H. Enhancement of Strain-Sensing Performance through Gas Phase Incorporation of Siloxane into Thermoplastic Polyurethane-Conducting Polymer Composite. *Macromol. Chem. Phys.* **2020**, 221, 2000155-2000164.

8. Janata, J.; Josowicz, M. Conducting Polymers in Electronic Chemical Sensors. *Nat. Mater.* **2003**, 2, 19-24.

9. Waghuley, S. A.; Yenorkar, S. M.; Yawale, S. S.; Yawale, S. P. Application of Chemically Synthesized Conducting Polymer-polypyrrole as a Carbon Dioxide Gas Sensor. *Sens. Actuators, B* **2008**, 128, 366-373.

10. Fernandez, F. D. M; Khadka, R.; Yim, J.-H. Highly Porous, Soft, and Flexible Vapor-phase Polymerized Polypyrrole–styrene–ethylene–butylene–styrene Hybrid Scaffold as Ammonia and Strain Sensor. *RSC Adv.* **2020**, 10, 22533-22541

11. Guerchouche, K.; Herth, E.; Calvet, L. E.; Roland, N. Loyez, C. Conductive Polymer Based Antenna for Wireless Green Sensors Applications. *Microelectron. Eng.* **2017**, 182, 46-52.

12. Zhang, W.; Zhao, B.; He, Z.; Zhao, X.; Wang, H.; Yang, S.; Wu, H.; Cao, Y. High-efficiency ITO-free Polymer Solar Cells Using Highly Conductive PEDOT:PSS/Surfactant Bilayer Transparent Anodes. *Energy Environ. Sci.*, **2013**, 6, 1956-1964.

13. Lövenich, W. PEDOT-Properties and Applications. *Polym. Sci. Ser. C* **2014**, 56, 135-143.

14. Wang, L. X.; Li, X. G.; Yang, Y. L. Preparation, Properties and Applications of Polypyrroles. *React. Funct. Polym.* **2001**, 47, 125-139.

15. Li, Z.; Ma, G.; Ge, R.; Qin, F.; Dong, X.; Meng, W.; Liu, T.; Tong, J.; Jiang, F.; Zhou, Y.; Li, K.; Min, X.; Huo, K.; Zhou, Y. Free-Standing Conducting Polymer Films for High-Performance Energy Devices. *Angew.Chem. Int. Ed.* **2016**, 55, 979-982.

16. Greco, F.; Zucca, A.; Taccola, S.; Menciassi, A.; Fujie, T.; Haniuda, H.; Takeoka, S.; Dario, P.; Mattoli, V. Ultra-thin Conductive Free-standing PEDOT/PSS Nanofilms. *Soft Matter*, **2011**, 7, 10642-10650.

17. Ni, D.; Song, H.; Chen, Y.; Cai, K. Free-standing Highly Conducting Pedot Films for Flexible Thermoelectric Generator. *Energy* **2019**, 170, 53-61.

18. Ni, D.; Chen, Y.; Song, H.; Liu, C.; Yang, X.; Cai, K. Free-Standing and Highly Conductive PEDOT Nanowire Films for High-performance All-solid-state Supercapacitors, *J. Mater. Chem. A* **2019**, 7, 1323-1333.

19. Nair, S.; Natarajan, S.; Kim, S. H. Fabrication of Electrically Conducting Polypyrrole-Poly(ethylene oxide) Composite Nanofibers. *Macromol. Rapid Commun.* **2005**, 26, 1599-1603.

20. Nair, S.; Hsiao, H.; Kim, S. H. Melt-Welding and Improved Electrical Conductivity of Nonwoven Porous Nanofiber Mats of Poly(3,4-ethylenedioxythiophene) Grown on Electrospun Polystyrene Fiber Template. *Chem. Mater.* **2009**, 21, 115-121.

21. Ali, M. A.; Wu, K. H.; McEwan, J.; Lee, J. Translated Structural Morphology of Conductive Polymer Nanofilmssynthesized by Vapor Phase Polymerization. *Synth. Met.* **2018**, 244, 113-119.

22. Evans, D.; Fabretto, M.; Mueller, M.; Zuber, K.; Short, R.; Murphy, P. Structure-directed Growth of High Conductivity Pedot from Liquid-like Oxidant Layers During Vacuum Vapor Phase Polymerization. *J. Mater. Chem.* **2012**, 22, 14889.

23. Brooke, R.; Fabretto, M.; Hojati-Talemi, P.; Murphy, P.; Evans, D. Evidence for 'Bottom Up' Growth During Vapor Phase Polymerization of Conducting Polymers. *Polymer* **2014**, 55, 3458-3460.

24. Brooke, R.; Cottis, P.; Talemi, P.; Fabretto, M.; Murphy, P.; Evans, D. Recent Advances in the Synthesis of Conducting Polymers from the Vapour Phase. *Prog. Mater. Sci.* **2017**, 86, 127-146.

25. Nodora, K. M. A.; Yim, J.-H. Elucidation of the Controversial Layer Growth Mechanism of Vapor Phase Polymerization in the Preparation of Conductive Poly(3,4-ethylenedioxythiophene)-SiO$_2$ Hybrid Films. *Adv. Mater. Interfaces* **2020**, 2000046.

26. Nakata, M.; Taga, M.; Kise, H. Synthesis of Electrical Conductive Polypyrrole Films by Interphase Oxidative Polymerization-Effects of Polymerization Temperature and Oxidizing Agents. *Polym. J.* **1992**, 24, 437-441.

27. Ansari, R. Polypyrrole Conducting Electroactive Polymers: Synthesis and Stability Studies. *E-J. Chem.* **2006**, 3, 186-201.

28. Lei, J.; Li, Z.; Lu, X.; Wang, W.; Bian, X.; Zheng, T.; Xue, Y.; Wang, C. Controllable Fabrication of Porous Free-standing Polypyrrole Films via Agas Phase Polymerization. *J. Colloid Interface Sci.* **2011**, 364, 555-560.

29. McFarlane, S. L.; Deore, B. A.; Svenda, N.; Freund, M. S. A One-Step, Organic-Solvent Processable Synthesis of PEDOT Thin Films via *In Situ* Metastable Chemical Polymerization. *Macromolecules* **2010**, 43, 10241-10245.

30. Shanthala, V. S.; Devi, S. N. S.; Murugendrappa, M. V. Optical Band Gap Studies of Polypyrrole Doped with Cuznfe2o4 Nano Particles. *Int. J. Sci. Res. Publ.* **2016**, 6(9), 21-27.

31. Khadka, R.; Yim, J.-H. Influence of Base Inhibitor and Surfactant on the Electrical and Physicochemical Properties of PEDOT-SiO$_2$ Hybrid Conductive Films. *Macromol. Res.* **2015**, 23, 559-565.

32. Ko, Y. S.; Yim, J.-H. Synergistic Enhancement of Electrical and Mechanical Properties of Polypyrrole Thin Films By Hybridization of SiO$_2$ with Vapor Phase Polymerization. *Polymer* **2016**, 93, 167-173.

33. Madl, C. M.; Kariuki, P. N.; Gendron, J.; Piper, L. F. J.; Jones Jr., W. E. Vapor Phase Polymerization of Poly(3,4-ethylenedioxythiophene) on Flexible Substrates for Enhanced Transparent Electrodes. *Synth. Met.* **2011**, 161, 1159-1165.